Structures of Horse Liver Alcohol Dehydrogenase Complexed with NAD+ and Substituted Benzyl Alcohols

ARTICLE *in* BIOCHEMISTRY · JUNE 1994

Impact Factor: 3.02 · DOI: 10.1021/bi00183a028 · Source: PubMed

3 AUTHORS, INCLUDING:

S Ramaswamy
Institute for Stem Cell Biology and Regenerat…

113 PUBLICATIONS **5,128** CITATIONS

SEE PROFILE

Structures of Horse Liver Alcohol Dehydrogenase Complexed with NAD^+ and Substituted Benzyl Alcohols[†,‡]

S. Ramaswamy,[*,§] Hans Eklund,[*,§] and Bryce V. Plapp[*,∥]

Department of Molecular Biology, Swedish University of Agricultural Sciences, Biomedical Center, Box 590, S-751 24 Uppsala, Sweden, and the Department of Biochemistry, The University of Iowa, Iowa City, Iowa 52242

Received November 17, 1993; Revised Manuscript Received March 4, 1994[⊛]

ABSTRACT: Structures of the enzyme complexed with NAD^+ and 2,3,4,5,6-pentafluorobenzyl alcohol were determined by X-ray crystallography at a resolution of 2.1 Å and to a refinement *R* value of 18.3% for a monoclinic ($P2_1$) form and to 2.4 Å and an *R* value of 18.9% for a triclinic crystal form. The pentafluorobenzyl alcohol does not react, due to electron withdrawal by the fluorine atoms. A structure with NAD^+ and *p*-bromobenzyl alcohol in the monoclinic form was also determined at 2.5 Å and an *R* value of 16.7%. The conformations of the subunits in the monoclinic and triclinic crystal forms are very similar. The dimer is the asymmetric unit, and a rigid body rotation closes the cleft between the coenzyme and catalytic domains upon complex formation. In the monoclinic form, this conformational change is described by a rotation of 9° in one subunit and 10° in the other. The pentafluoro- and *p*-bromobenzyl alcohols bind in overlapping positions. The hydroxyl group of each alcohol is ligated to the catalytic zinc and participates in an extensive hydrogen-bonded network that includes the imidazole group of His-51, which can act as a base and shuttle a proton to solvent. The hydroxymethyl carbon of the pentafluorobenzyl alcohol is 3.4 Å from C4 of the nicotinamide ring, and the *pro-R* hydrogen is in a good position for direct transfer to C4. The *p*-bromobenzyl alcohol may react after small rotations around single bonds of the alcohol. These structures should approximate the active Michaelis–Menten complexes.

Horse liver alcohol dehydrogenase (EE isoenzyme, EC 1.1.1.1) is an NAD-dependent enzyme with a broad substrate specificity, being active on a variety of primary, secondary, branched, and cyclic alcohols (Sund & Theorell, 1963). The enzymatic mechanism and structures of various complexes have been extensively studied (Brändén et al., 1975; Eklund & Brändén, 1987; Pettersson, 1987). The catalytic reaction is ordered, with NAD^+ or NADH binding to free enzyme when primary alcohols and aldehydes, such as ethanol and acetaldehyde or benzyl alcohol and benzaldehyde, are the substrates (Wratten & Cleland, 1963; Shearer et al., 1993). The enzyme has a molecular weight of 80 000 and is a dimer of two identical subunits, each of which has a coenzyme-binding and a catalytic domain. The coenzyme-binding domains have structures similar to those found in several other NAD-dependent dehydrogenases (Rossmann et al., 1975), and they form a 12-stranded β-pleated sheet structure that makes up the central core of the dimer (Eklund et al., 1976). The two active sites are in clefts between the coenzyme-binding core and the catalytic domains. Substrates bind in a hydrophobic pocket in the cleft with their oxygen atoms ligated to the zinc atoms of the catalytic domains. When coenzymes bind, the active site clefts close up by a rigid body rotation of the catalytic domains toward the coenzyme-binding domains (Eklund & Brändén, 1979; Eklund et al., 1981). Relative to the apoenzyme, the rotation of the catalytic domains is about 10° for the complex with NADH and dimethyl sulfoxide in the triclinic crystal form (Colonna-Cesari et al., 1986). The apo- and holoenzyme structures were determined at 2.4- and 2.9-Å resolution, respectively. The conformational change and the catalytic mechanism should be studied further at higher resolution with additional complexes.

The three-dimensional structure of a complex with NAD and *p*-bromobenzyl alcohol was determined at 2.9-Å resolution for a triclinic crystal form (Eklund et al., 1982). This structure has been used as a model for the active enzyme–substrate complex, but the *pro-R* hydrogen of substrate was oriented away from the nicotinamide ring in the observed mode of binding so that rotation around single bonds of the substrate appeared to be required for direct hydrogen transfer. The complex was formed with good substrates at kinetically saturating levels so that the composition of the complex should reflect the internal equilibrium on the surface of the enzyme, which favors NAD^+–alcohol over NADH–benzaldehyde (Eklund et al., 1982; Shearer et al., 1993). However, it has also been suggested that the complex contains NADH and may be an abortive complex with the alcohol (Bignetti et al., 1979; Schneider et al., 1985). This complex could form as the enzyme slowly oxidizes benzaldehyde to benzoic acid (Anderson & Dahlquist, 1980), which removes the aldehyde that maintains the internal equilibrium of reactants bound to the enzyme (Shearer et al., 1993). Thus, structures of complexes with substrate analogs that would not be oxidized should be determined at high resolution.

The unreactive analog of ethanol, 2,2,2-trifluoroethanol, forms a tight ternary complex with alcohol dehydrogenase and NAD^+ (Plapp et al., 1978). 2,3,4,5,6-Pentafluorobenzyl alcohol also is not oxidized and is a competitive inhibitor against ethanol with a K_i value of 3 μM (Shearer et al., 1993). It forms a tight complex that should resemble the Michaelis–Menten complex. The fluorine atoms have nonspherical van der Waals radii of 1.30 and 1.38 Å (Nyburg & Faerman, 1985), in between those of hydrogen and oxygen, so that steric interactions are similar to those of unsubstituted benzyl alcohol.

[†] This work was supported by the Natural Science Research Council of Sweden (H.E.) and United States Public Health Service Grant AA00279 (B.V.P.).

[‡] The coordinates have been deposited in the Brookhaven Protein Data Bank (entry 1HLD).

[*] Address correspondence to any of the authors.

[§] Swedish University of Agricultural Sciences.

[∥] The University of Iowa.

[⊛] Abstract published in *Advance ACS Abstracts,* April 15, 1994.

0006-2960/94/0433-5230$04.50/0

In this work, structures of the complex with NAD^+ and pentafluorobenzyl alcohol were determined in a new monoclinc crystal form and in the triclinic form. Furthermore, a structure of the complex with NAD and *p*-bromobenzyl alcohol was also determined in the monoclinic form. Both complexes show the coenzyme and alcohol bound in positions suitable for hydrogen transfer.

EXPERIMENTAL PROCEDURES

Crystallization. The crystals were prepared under the conditions described previously (Plapp et al., 1978) with the following modifications. Horse liver alcohol dehydrogenase EE isoenzyme from Boehringer Mannheim was recrystallized from 10 mM sodium phosphate buffer, pH 7.0, with 10% ethanol, and the crystals were dissolved in a buffer containing about 0.5 M KCl and dialyzed against 50 mM ammonium *N*-[tris(hydroxymethyl)methyl]-2-aminoethanesulfonate buffer, pH 6.7 (measured at 25 °C, pH 7.0 at 5 °C) until the KCl and ethanol were removed. The solution was clarified by centrifugation and sterilized by filtration. The concentration of protein was determined by UV absorption (A_{280} = 0.455/cm for 1 mg/mL). The enzyme was homogeneous by gel electrophoresis and chromatography, and 95% of the enzyme subunits were able to bind NAD^+ as determined by titration in the presence of 10 mM pyrazole (Theorell & Yonetani, 1963). Aliquots of 1 mL of 10 mg/mL of the enzyme in washed dialysis bags were placed into solutions containing 10 mL of 50 mM ammonium *N*-[tris(hydroxymethyl)methyl]-2-aminoethanesulfonate, pH 6.7, and 0.7 mM NAD^+ and either 8 mM 2,3,4,5,6-pentafluorobenzyl alcohol (Aldrich) or 10 mM *p*-bromobenzyl alcohol. Crystals formed at 5 °C after addition of about 10% 2-methyl-2,4-pentanediol, which was purified by treatment with activated charcoal, and were brought to a final concentration of about 25% diol before mounting in glass capillaries. X-ray data were collected 9–12 months after enzyme preparation. For the pentafluorobenzyl alcohol complex, the spectrum of the outer dialyzate and of crystals dissolved in phosphate buffer with 1 mM fluoroalcohol showed that NAD^+, and not NADH, was present.

Data Collection. X-ray data on a single triclinic crystal (unit cell dimensions of a = 52.3 Å, b = 44.5 Å, c = 93.9 Å, α = 104.7°, β = 102.2°, and γ = 70.6°) were collected at 4 °C with a Xentronics multiwire area detector (Nicolet) mounted on a Rigaku rotating anode with 0.1° oscillation frames and processed with the BUDDHA program (Blum et al., 1987). The data for the monoclinic crystals (unit cell dimensions of a = 51.1 Å, b = 180.7 Å, c = 44.3 Å, and β = 108.0°) were collected at 4 °C on an *R* axis II imaging plate system with a Rigaku rotating anode from two crystals of the complex with pentafluorobenzyl alcohol and one crystal of the complex with *p*-bromobenzyl alcohol. The data were further processed and scaled with the Rotavata and Agrovata programs in the CCP4 program package (Daresbury, England), and the results are summarized in Table 1.

Refinement. Structures were refined with the program XPLOR (Brünger et al., 1987) using structural parameters from Engh and Huber (1991). The program O was used for computer graphics modeling (Jones et al., 1991). The asymmetric unit in each crystal form is the dimer, and the subunits were refined independently. Phases for the initial triclinic model were calculated from the structure of the enzyme–NADH–dimethyl sulfoxide complex determined at 2.9 Å and with an *R* value of 22% (Eklund et al., 1984) with the dimethyl sulfoxide removed. Phases for the monoclinic structure were derived by molecular replacement using XPLOR (Brünger et al., 1987). The starting model was the structure of the enzyme with bound pentafluorobenzyl alcohol in the triclinic crystal form, which had been partially refined initially. The molecule was unambigously positioned by using the cross rotation function calculation, followed by Patterson correlation refinement, which gave a clear solution that was used for the translation function. Simulated annealing and positional refinement with XPLOR, alternating with manual modeling, readily improved the structure. No charges were assigned to the two zinc atoms and their ligands, amino acid side chains, the pentafluoroalcohol, and the NAD during refinement. Water molecules were added as the refinement progressed, and densities of appropriate magnitude ($\sigma > 1$) and position (such as hydrogen-bonded distance to polar residues) were located in difference Fourier maps. At one stage the *R* value was 23.5% and did not improve further, even though the electron density image was relatively good. After anisotropic scaling of F_o against F_c using XPLOR, refinement eventually decreased the *R* value to 18.3%.

The starting model for the structure with *p*-bromobenzyl alcohol was the refined monoclinic structure including the water molecules but without the pentafluorobenzyl alcohol. After 200 cycles of conventional positional refinement, the $2|F_o| - |F_c|$ and $|F_o| - |F_c|$ maps clearly showed the positions of the benzene rings and the bromine atoms. The next cycle of refinement included all the atoms of the *p*-bromobenzyl alcohol except the alcohol oxygen, in order to define the density unambiguously. Refinement of the protein and the bromobenzyl alcohol as separate rigid bodies was followed by simulated annealing at room temperature and another round of conventional positional refinement. The difference maps calculated at this stage clearly indicated the positions for the oxygen atoms in both subunits. The coordinates for the monoclinic complexes have been deposited in the Protein Data Bank at Brookhaven with entry name 1HLD.

Table 1: Data Collection and Characteristics of the Refined Structures

NAD–alcohol complex	pentafluorobenzyl		*p*-bromobenzyl
space group	$P2_1$	$P1$	$P2_1$
total reflections measured	65557	26542	40053
R_{merge} (%)[a]	5.5	8.4	8.0
non-zero reflections used	37152	23629	18605
% completeness	84	76	72
resolution (Å)	8.0–2.1	8.0–2.4	8.0–2.5
R value (%)[b]	18.3	18.9	16.7
bond distances[c]	0.010	0.012	0.010
bond angles[c]	1.7	1.9	1.7
dihedral angles[c]	25.4	26.5	25.5
water molecules	394	298	394[d]

[a] R_{merge}, $(\Sigma|I - \langle I\rangle|)/\Sigma\langle I\rangle$. [b] *R* value, $(\Sigma||F_o| - k|F_c||)/\Sigma|F_o|$, where k is a scale factor. [c] Root-mean-square (rms) deviations from ideal geometry of the final model. [d] The monoclinic complex with pentafluorobenzyl alcohol was used for refinement, so the structure has the same number of water molecules.

RESULTS AND DISCUSSION

Tertiary Structures. Both monoclinic and triclinic crystals of the ternary complexes with NAD^+ and 2,3,4,5,6-pentafluorobenzyl alcohol or *p*-bromobenzyl alcohol form under the same conditions, as was found for the ternary complex with NADH and dimethyl sulfoxide (Eklund et al., 1981). This provides the opportunity to compare structures of molecules that are packed differently in the unit cell. Preliminary studies were made on a monoclinic complex (Samama, 1979), and the refined structure of the triclinic form was described at 2.9 Å with an *R* value of 22% (Eklund

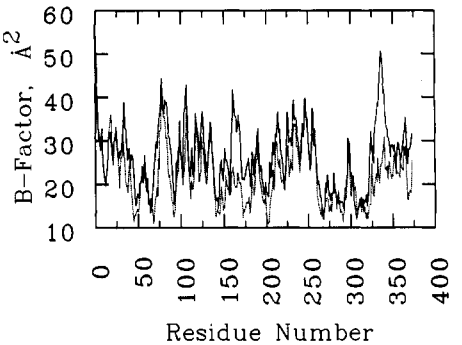

FIGURE 1: Temperature factors for the peptide backbone of the monoclinic complex with NAD and pentafluorobenzyl alcohol. The averages for the main chain atoms of each residue are given for subunit 1 (dotted line) and subunit 2 (solid line).

et al., 1984). Now both structures have been refined at higher resolution. The final models have good structural parameters (Table 1). Since the monoclinic complex with pentafluorobenzyl alcohol has now been determined to the best resolution, it will serve as the basis for the following discussion.

Almost all residues are located in well-defined density in the Fourier maps. A few polar side chains (11 of 748 residues) have weak density and possibly multiple conformations, but the alternative positions were not refined. The residues at the active site are well-defined. Temperature factors are low for most main chain atoms, indicating that few residues are in flexible regions (Figure 1). The major differences in temperature factors between subunit 1 and subunit 2 are around residues 161 and 338. These two regions are topological neighbors and are on the surface. This region in subunit 1 interacts directly with a symmetry-related molecule via some hydrogen bonds between side chains of subunit 1 and main chain atoms of the related subunit. The same region in subunit 2 interacts only with the solvent. Thus, packing of the molecules in the crystal lattice appears to affect the flexibility and temperature factors of this region.

The structural characteristics evaluated with PROCHECK (Laskowski et al., 1992) are consistent with highly refined structures at this resolution. For example, the Ramachandran plot in Figure 2 shows that most residues have low energy conformations for the peptide backbone. A notable outlier in both subunits of all the structures is Cys-174 (ϕ about −164° and ψ about −84°), which also has similar unusual main chain torsion angles in the orthorhombic form of the apoenzyme (Jones et al., unpublished results). The active site zinc atom is ligated to the sulfur of Cys-174, and this residue is at the juncture of a 3_{10} and an α helix, which connect the catalytic and coenzyme-binding domains.

The enzyme has different conformations in the free and ternary complexes, due to movement of catalytic domains toward the coenzyme-binding domains (Eklund et al., 1981). Superpositioning the coenzyme-binding domains of the orthorhombic apoenzyme and the triclinic NADH–dimethylsulfoxide complex showed that Cα atoms of some residues in the catalytic domains moved by as much as 7 Å [Figure 4 from Eklund et al. (1981)]. This conformational change can be described by a rigid body rotation of 10° for the catalytic domains around a hinge that includes residues 173–175 and 318–321 (Colonna-Cesari et al., 1986). Since the asymmetric unit in both crystal forms is the dimer, the subunits of the ternary complexes could differ in the relative positions of the domains. For the monoclinic form, subunit 1 can be superpositioned on subunit 2 (based only on the Cα atoms) with an rms difference of 0.24 Å, indicating that the two

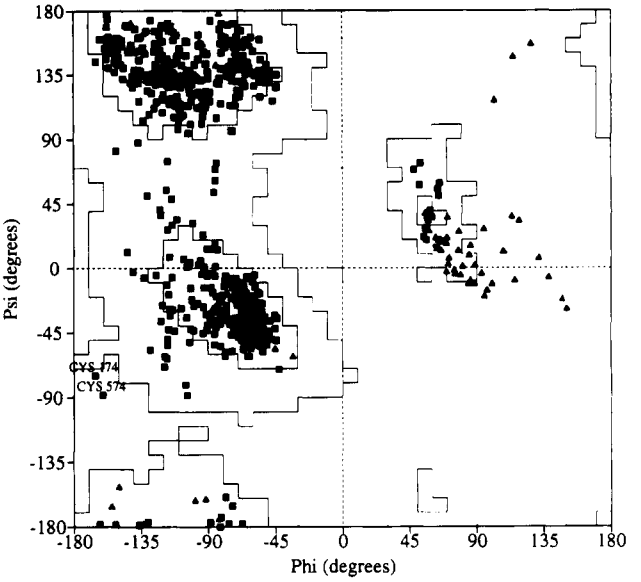

FIGURE 2: Ramachandran plot for both subunits of the monoclinic complex with NAD and pentafluorobenzyl alcohol. PROCHECK (Laskowski et al., 1993) was used for the calculation. The contours correspond to the "most favored" and "additional allowed regions". Glycine residues are indicated by (▲). Cys-574 is Cys-174 in subunit 2.

Table 2: Comparisons of Structures of the Triclinic and Monoclinic Complexes with Pentafluorobenzyl Alcohol[a]

structures compared	rms differences (Å)
monoclinic subunits 1 and 2	0.24
monoclinic coenzyme binding domains 1 and 2	0.20
monoclinic catalytic domains 1 and 2	0.22
monoclinic catalytic domains after superposing coenzyme domains	0.38
triclinic subunits 1 and 2	0.30
triclinic coenzyme binding domains 1 and 2	0.28
triclinic catalytic domains 1 and 2	0.33
monoclinic and triclinic dimers	0.33
monoclinic and triclinic coenzyme domains	0.25–0.26
monoclinic and triclinic catalytic domains	0.31–0.32

[a] Residues 5–174 and 316–374 were included in the catalytic domain and 176–314 in the coenzyme-binding domain. Root-mean-square (rms) differences for Cα atoms were computed with the program RMSPDB, written by Gerard J. Kleijwegt, University of Uppsala.

subunits are very similar (Table 2). However, superpositioning the coenzyme binding domains (residues 176–314, with an rms difference of 0.20 Å) leads to an rms difference of 0.38 Å between the Cα atoms of the catalytic domain. Examination of the differences arising from this comparison (Figure 3) shows that the largest differences (about 1 Å) are for residues on the end of the catalytic domain that move the most during the conformational change. For the monoclinic complexes, the catalytic domain of subunit 1 has rotated by 9° and that of subunit 2 by 10°, relative to the catalytic domains of the apoenzyme. The rotation angle after superpositioning the subunits as described in Figure 3 is 1°. The results suggest that a cooperative movement leads to a more closed catalytic region in subunit 2 than in subunit 1. The differences in the monoclinic subunits may result from crystal packing, as the catalytic domain of subunit 1 has many direct interactions with the neighboring symmetry-related molecules, in contrast to subunit 2, which has few such interactions.

The subunits in the triclinic pentafluorobenzyl alcohol complex did not show signficant asymmetry. The dimers from the triclinic and monoclinic forms can be superpositioned with a rms difference of 0.33 Å, indicating that the conformations

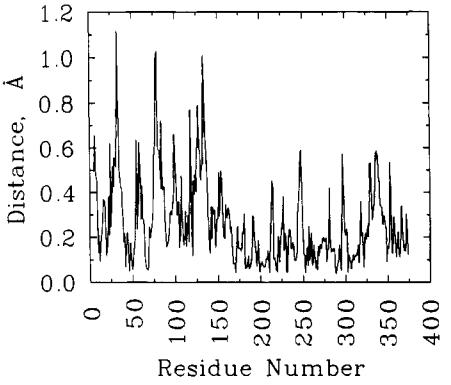

FIGURE 3: Comparison of conformations of subunits of the monoclinic complex with pentafluorobenzyl alcohol. The distances between equivalent Cα atoms in the two subunits were calculated with RMSPDB after superpositioning the coenzyme binding domains.

Table 3: Buried Waters in the Monoclinic Complex with Pentafluorobenzyl Alcohol

sub1	sub2	interactions (as in subunit 1)
127	21	N 94; N 93; WAT 128
128	22	O 173; N 93; 91 O; WAT 127, 129
129	23	N 69; O 67; O 91; WAT 128
130	24	N 67; N 68; O 44; OD1 49
131	25	N 370; O 368; O 45; WAT 132
132	26	OG 367; O 358; OG 370; WAT 131
133	27	NH1 369; O2PA NAD; O 368; N 202
201	309	ND1 139; O 151; O 143
212	333	O 12; O 63; N 65
109	366	N 320; OG 182; O 317
135	367	N 204; N 201; O 268; O2PN NAD
108	368	O 275; NE1 314; OG 289

are very similar. However, when the coenzyme-binding domains of the dimers for the two crystal forms were superimposed, the catalytic domains of the triclinic and monoclinic subunits were slightly different. The significance of these differences cannot be evaluated at the current resolution.

The refinement of the monoclinic complex located many water molecules bound to the surface of the enzyme. In addition, there are a number of waters buried within the protein, not directly connected to bulk solvent. The accessible surface area (Lee & Richards, 1971) of the protein was computed for all solvent molecules using the CCP4 suite of programs. When these waters were examined visually, 12 buried waters, with accessible areas of less than 2 Å^2, were found in each subunit. They are listed with their interactions in Table 3. None of the waters is buried in a strictly nonpolar cavity, as expected (Matthews, 1993). Many of these waters provide hydrogen-bonding interactions for peptide units that are not in regular secondary structures and thus can have structural roles (Teeter, 1991). One constellation, which is near the active site, contains three waters hydrogen bonded together and interacting with main chain atoms (Figure 4).

Coenzyme Binding. The coenzyme is bound in the same position and with the same amino acid residues described previously (Eklund et al., 1984) except that additional water molecules have now been located that form contacts with the pyrophosphate oxygens (Figures 5 and 6). One oxygen (O2PA) is connected by one water molecule to the guanidino NH1 of Arg-369, 202 N, and 368 O, and by a second water to the ε-amino group of Lys-228 and 367 O. Another oxygen (O2PN) binds 203 N and is connected by one water to 201 N, 204 N, and 268 O. Contacts between proteins and nucleotides mediated by water molecules have been described in DNA–protein interactions and in refined dehydrogenase structures (Steitz, 1990; Skarżyński et al., 1987; Birktoft et al., 1989). The water molecules may modulate binding affinity by decreasing the strength of ionic interactions and by providing a more flexible binding environment that ultimately determines the observed rates of association and dissociation.

The nicotinamide ring of the coenzyme is within van der Waals distance of four oxygens, provided by Thr-178 OG, Ser-48 OG, 292 O, and the O of pentafluorobenzyl alcohol. These oxygens may influence the reactivity of the nicotinamide ring, as discussed for bacterial dihydrofolate reductase (Filman et al., 1982). The carboxyamido group is hydrogen-bonded to main chain atoms and twisted out of the plane of the pyridine ring, as described previously (Eklund et al., 1984).

Substrate Binding Pocket. The structures of the protein and coenzymes in the monoclinic complexes with pentafluorobenzyl alcohol and *p*-bromobenzyl alcohol are the same, but the positions of the benzyl alcohols are slightly different. The locations of the pentafluorobenzyl alcohol are very well-defined in electron density, due especially to the electrons from the fluorines (Figure 7A). The bromines and planes of the *p*-bromobenzyl alcohols are also clearly positioned (Figure 7B). The hydroxymethyl groups of these alcohols are located in good density with the oxygens ligated to the catalytic zinc. In the other ternary complexes of the enzyme in the triclinic crystal form, with dimethyl sulfoxide, *trans*-4-(*N*,*N*-dimethylamino)cinnamaldehyde, pyrazole, or *p*-bromobenzyl alcohol,

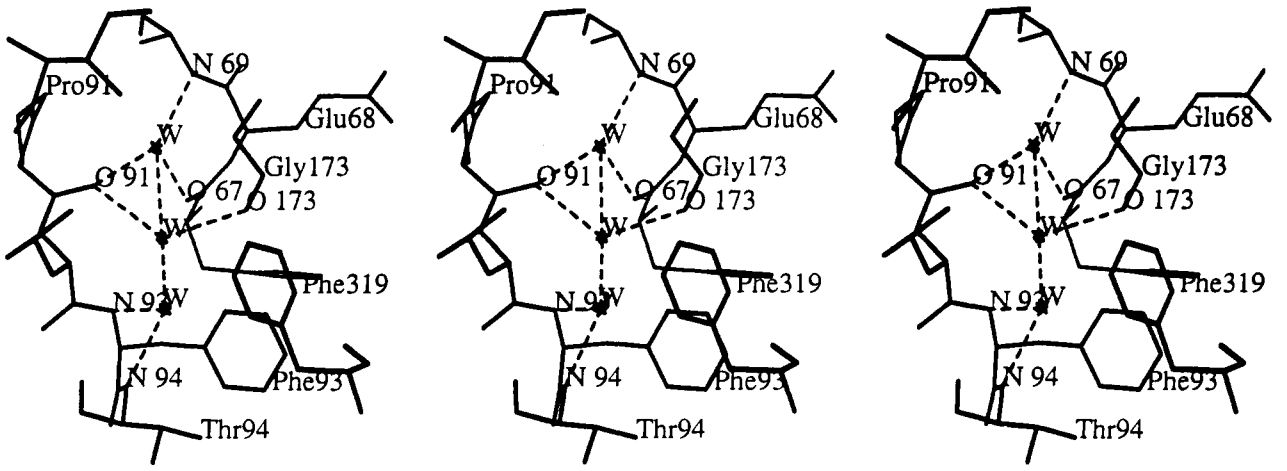

FIGURE 4: Cluster of buried waters. These waters are blocked off from the substrate binding pocket by Phe-93, which is near Phe-319. Four different peptide segments are shown. Hydrogen bonds are indicated by dashed lines.

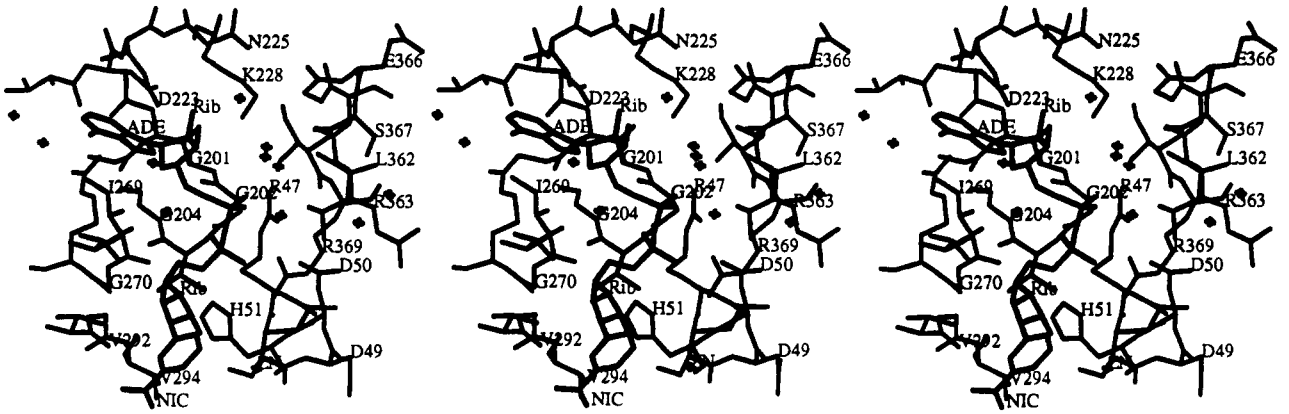

FIGURE 5: Stereoscopic view of coenzyme binding. Water molecules appear as crosses, and interacting residues are labeled.

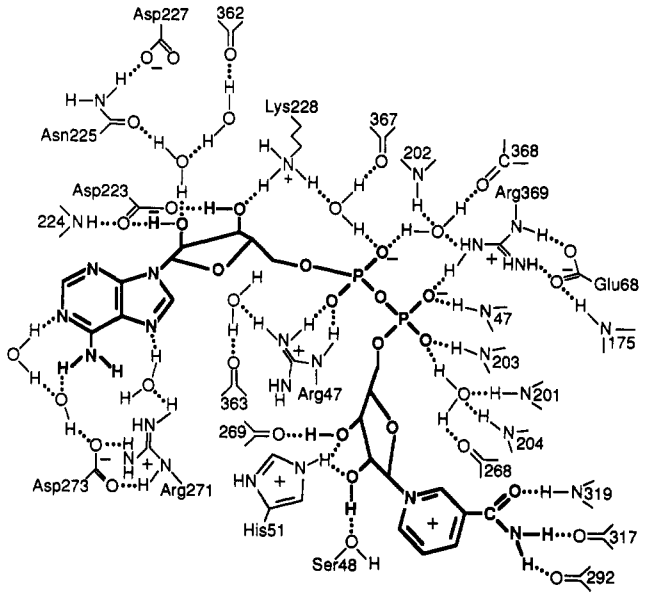

FIGURE 6: Diagram of coenzyme binding. The interactions identified in Figure 5 are shown.

Table 4: Geometry around the Catalytic Zincs in the Monoclinic Complex with NAD and Pentafluorobenzyl Alcohol

atoms		residue	distances (Å) subunit 1	distances (Å) subunit 2
Zn	SG	Cys-46	2.2	2.2
Zn	NE2	His-67	2.2	2.2
Zn	SG	Cys-174	2.3	2.2
Zn	O1	PFB[a]	2.0	2.0

atoms			angles (deg) subunit 1	angles (deg) subunit 2
46 SG	Zn	174 SG	129	122
46 SG	Zn	67 NE2	115	111
46 SG	Zn	O1 PFB	115	113
67 NE2	Zn	174 SG	104	112
67 NE2	Zn	O1 PFB	91	94
174 SG	Zn	O1 PFB	95	101

[a] PFB is 2,3,4,5,6-pentafluorobenzyl alcohol.

the ligand is also directly bound to the catalytic zinc (Eklund et al., 1981, 1982, 1984; Cedergren-Zeppezauer et al., 1982). The geometry of ligation to the catalytic zinc is similar in both subunits and in the other complexes (Table 4).

The positions of the substituted benzyl alcohols in the monoclinic complexes are compared in Figure 8. The benzene rings of the two alcohols are coplanar, but the rings are rotated by about 40° around an axis perpendicular to the plane of the

Table 5: Contacts between Atoms of the Benzyl Alcohols and the Enzyme and Coenzyme in the Monoclinic Complexes[a]

atoms	distances (Å) to residue, atoms			
	Pentafluorobenzyl Alcohol			
O1	2.6 Ser48 OG	3.1 His67 NE2	3.2 NAD C5N	2.0 Zn
C7	3.4 NAD C4N	3.5 Phe93 CZ		
HR	2.5 NAD C4N			
C1	3.3 Ser48 OG	4.0 Phe93 CZ		
C2	3.6 Val294 CG2	4.0 Ser48 OG	4.0 NAD C3N	
C3	3.4 Val294 CG2	3.7 Leu116 CD2		
C4	3.7 Leu116 CD2	4.0 Leu57 CD2		
C5	3.7 Leu57 CD2	4.0 Ser48 CB		
C6	3.4 Ser48 CB	4.0 Leu141 CD1		
F2	2.8 NAD C7N	3.6 Val294 CG2	3.9 Ile318 CD1	
F3	3.2 Val294 CG2	3.4 Ile318 CD1	3.8 Leu116 CD2	
F4	3.6 Leu57 CD1	3.6 Leu116 CD1	3.2 OH2	
F5	3.2 Leu57 CD2	3.4 Phe140 CZ	3.6 Leu141 CD1	
F6	3.1 His67 NE2	3.1 Ser48 CB	3.5 Leu141 CD2	
	p-Bromobenzyl Alcohol			
O1	2.8 Ser48 OG	3.2 His67 NE2	3.2 NAD C5N	2.2 Zn
C7	3.3 His67 NE2	3.6 Ser48 OG	3.7 Phe93 CE2	4.3 NAD C4N
HR	4.7 NAD C4N			
C1	3.5 Ser48 OG	3.8 Phe93 CE2		
C2	3.2 NAD O7N	3.4 NAD C3N		
C3	3.3 Val294 CG2	3.5 NAD O7N	3.9 Ile318 CD1	
C4	3.5 Val294 CG2	3.9 Leu116 CD2		
C5	3.9 Leu57 CD2	3.9 Leu116 CD2		
C6	3.9 Ser48 CB	4.0 Leu141 CD1		
Br	3.8 Val294 CG2	4.1 Leu116 CD2	3.0 OH2	

[a] The methylene carbon of benzyl alcohol is labeled C7 and the *pro-R* hydrogen H*R*.

rings. The binding of *p*-bromobenzyl alcohol is similar to that found in the triclinic form determined at 2.9 Å (Eklund et al., 1982), but the higher resolution defines the planes of the benzene rings better. The bromine fits into the extended pocket. The differences in binding between the pentafluorobenzyl and *p*-bromobenzyl alcohol complexes could arise because of the fluorine and bromine substitutions. The fluoroalcohol is close to the same size as benzyl alcohol, so that large steric interactions are not being introduced with the unreactive substrate analog. The average van der Waals contact radius of 1.34 Å for fluorine is similar to hydrogen with a radius of 1.20 Å (Bondi, 1964), which means that the distances from fluorines to other atoms in the substrate pocket are shorter than for distances between C, N, or O atoms. The distances are listed in Table 5. Binding of the benzyl alcohols in the two different subunits of the two different crystal forms is very similar, but there are some differences of a few tenths of angstrom.

An aldehyde could also be accommodated by the electron density maps, but the enzyme does not oxidize the pentafluorobenzyl alcohol, and only the alcohol was found in the

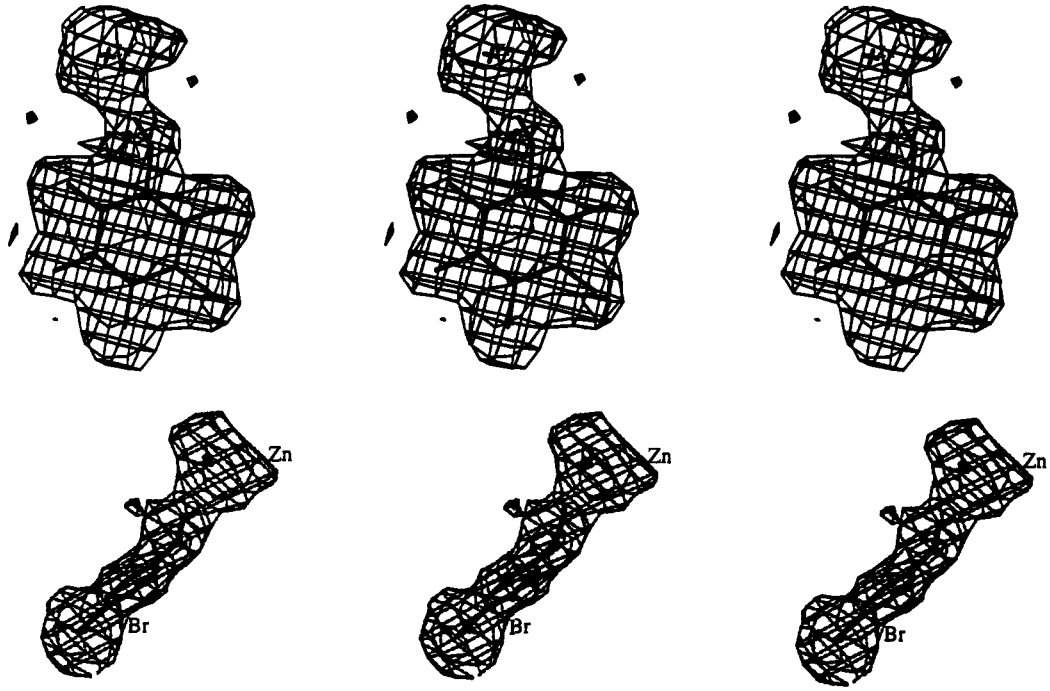

FIGURE 7: Binding of benzyl alcohols in monoclinic complexes. The electron densities from $2|F_o| - |F_c|$ Fourier maps, calculated with the final coordinates, are presented for subunit 1 for both complexes. Both subunits had similar densities. The contour level was at 1σ, and the bromine atoms were in density at 5σ. (A, top) Pentafluorobenzyl alcohol. (B, bottom) *p*-Bromobenzyl alcohol.

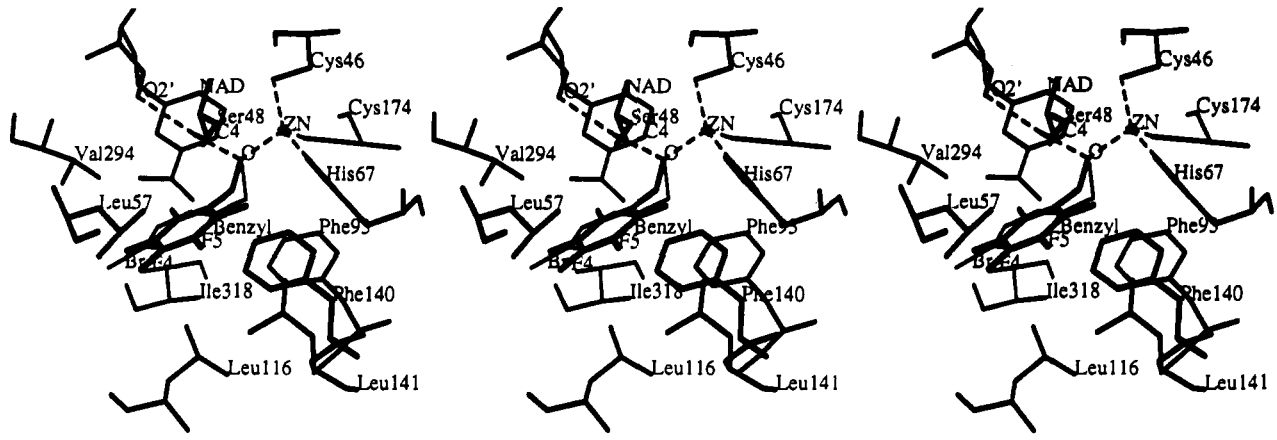

FIGURE 8: Comparison of the binding modes for pentafluorobenzyl alcohol (thick lines, *F4* and *F5*) and *p*-bromobenzyl alcohol (thin lines, *Br*). The oxygens of the alcohols are ligated to the catalytic zinc. Hydrogen bonds and zinc ligands are indicated by the dashed lines.

crystallization mixtures. With 10 mg/mL enzyme, 1 mM NAD^+ and 1 mM alcohol at pH 7, hydrogen transfer with 2-fluorobenzyl alcohol was 2% of the rate with benzyl alcohol, but no activity with pentafluorobenzyl alcohol was detected. The *p*-bromobenzyl alcohol could be oxidized to the aldehyde, but the internal equilibrium favors alcohol, and dismutation would lead to the formation of the enzyme–NADH–alcohol complex and *p*-bromobenzoic acid (Eklund et al., 1982; Shearer et al., 1993). At this resolution the difference between NAD^+ and NADH cannot be observed, but there is not sufficient electron density to accommodate a carboxyl group.

Proton Relay System. The hydroxyl groups of the benzyl alcohols are ligated to the catalytic zinc and linked to the imidazole group of His-51 through the hydrogen-bonded system containing the hydroxyl groups of Ser-48 and the nicotinamide ribose, as shown before (Eklund et al., 1982). This system is suited for relaying a proton from the alcohol to solvent during dehydrogenation. The present higher resolution studies support the previous conclusions and show that His-51 participates in a more extensive hydrogen-bonded system that is linked by a water molecule to the carboxyl group of Asp-50 and the hydroxyl group of Ser-54 (Figures 9 and 10). Although the positions of hydrogen atoms cannot be determined from the electron density maps, we surmise that ND1 of His-51 donates a hydrogen to the water molecule, which is donating both of its hydrogens to its neighbors, as the hydroxyl group of Ser-54 donates its hydrogen to the carbonyl oxygen of Asp-50. NE2 of His-51 is close enough to form hydrogen bonds to both the O2′ and O3′ hydroxyl groups of the nicotinamide ribose, but the O3′ hydroxyl must donate its hydrogen to the carbonyl oxygen of Ile-269. Thus, one hydrogen is shared by NE2 of His-51 and the ribose oxygens, as in bifurcated hydrogen bonds observed in other proteins (Baker & Hubbard, 1984). In subunit 2, the distance between NE2 and O2′ is 2.9 Å and that between NE2 and O3′ is 3.0 Å, whereas in subunit 1 the distances are 3.3 and 3.1 Å, respectively. In both subunits the groups are oriented for more linear hydrogen bonds between NE2 and O3′, but rotation around the Cα–Cβ (χ_1) bond of His-51 can readily move NE2 closer to O2′. Movement of the histidine may

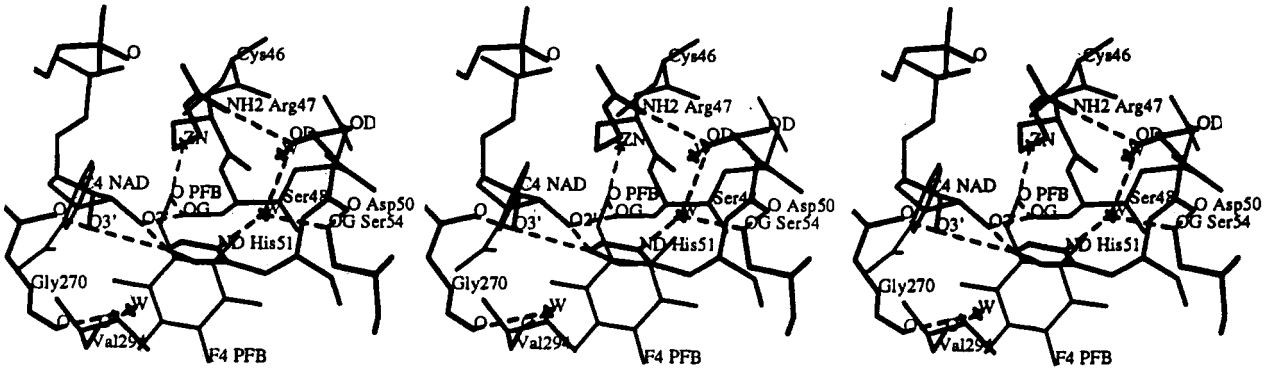

FIGURE 9: Extended hydrogen-bonded system linking the oxygen of the substrate to solvent. The system (subunit 2) includes the O of pentafluorobenzyl alcohol (*PFB*), OG of Ser-48, O2′ of NAD, the imidazole of His-51, a water, OG of Ser-54, OD1, and O of Asp-50. The carboxyl group of Asp-50 interacts with the guanidino group of Arg-47 and an additional water. Other waters (not shown) in the cleft are exposed to bulk solvent.

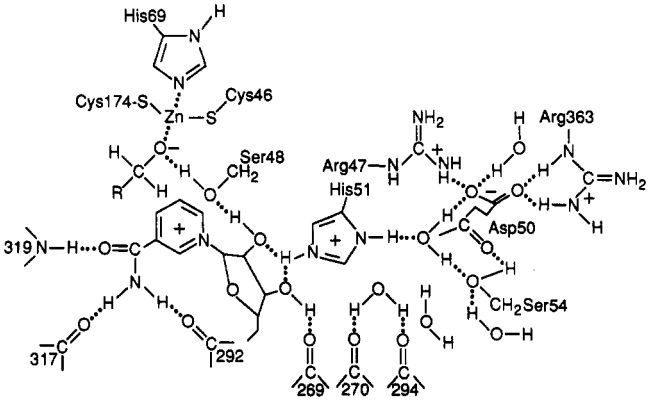

FIGURE 10: Interpretation of the hydrogen-bonded system and its role in proton transfer. The interactions shown in Figure 9 are represented.

facilitate catalytic dynamics, as suggested for serine proteases (Meyer, 1992).

During dehydrogenation, the alcohol loses its proton and forms the alkoxide, apparently facilitated by the proton relay system. The zinc stabilizes the alcohol as an alkoxide and contributes an estimated factor of 100-fold to the redox reaction (Creighton et al., 1976). The imidazole of His-51 contributes about 10-fold to activity as estimated from the decrease in activity upon substitution with a Gln (Ehrig et al., 1991; Park, 1991). Inspection of the system suggests that the hydroxyl group of the benzyl alcohol has retained the proton (as ROH) and His-51 is neutral or that the benzyl alcohol has lost its hydrogen to form the alkoxide (RO^-) and His-51 is diprotonated, as illustrated in Figure 10. The microscopic pK values for His-51 in the ternary complexes with benzyl alcohol and the substituted derivatives have not been directly established, but various experiments give macroscopic estimates consistent with the neutral or zwitterionic states. Steady-state kinetic studies with a modified enzyme or transient studies with native enzyme show that the rate of benzyl alcohol oxidation is most rapid above a pK value of 8.4 or 6.4 (Dworschack & Plapp, 1977; Kvassman & Pettersson, 1978). Furthermore, the position of the internal equilibrium (E–NAD^+–benzyl alcohol $\rightleftharpoons$ E–NADH–benzaldehyde) exhibits a complex pH dependence with pK values of 6.5 and 8.1 (Shearer et al., 1993). Since the hydrogen-bonded system contains two ionizable groups, the alcohol and His-51, microscopic values can only be assigned when additional evidence is obtained.

The transient oxidation of ethanol occurs twice as fast in D_2O as in H_2O, an inverse solvent isotope effect (Sekhar & Plapp, 1990). The results can be explained by a ground state fractionation factor (ϕ_R) of 0.37 for a negatively charged alkoxide in a nonaqueous environment and a transition state factor (ϕ_T) of 0.73 for a partially charged state. Cleland (1992) has suggested that "low-barrier" hydrogen bonds, where the O to O distances are relatively short, could account for the fractionation factors. The observed structure of the enzyme complex is consistent with these explanations.

After accepting a proton to become diprotonated (Figure 10), His-51 could relay the proton to solvent by different mechanisms. The water molecule hydrogen bonded to ND1 of His-51 could accept the proton and transfer it to a nearby water. Alternatively, a rotation of about 20° around the Cα–Cβ (χ_1) bond of His-51 moves NE2 away from its interactions with the hydroxyl groups of the nicotinamide ribose and toward a water molecule that is in the channel leading to the surface of the protein. The water molecule is hydrogen-bonded to the carbonyl oxygens of residues 270 and 294 and is close to other identified waters. Thus, the protonated imidazole group could easily donate a proton to water molecules which are connected to bulk solvent.

Hydride Transfer. In the observed binding mode for the monoclinic and triclinic complexes with pentafluorobenzyl alcohol, the methylene C of the alcohol (C7) is 3.4 Å from C4 of the nicotinamide ring, the oxygen of the alcohol is about 3.2 Å from C5 of the nicotinamide ring, and the *pro-R* hydrogen is pointing almost directly toward C4 of the NAD^+ (Figure 11). The direction of the bond between C7 and the donor *pro-R* hydrogen deviates from the direction to the position for a *pro-R* hydrogen on C4 of the nicotinamide ring by about 40°. This complex appears to represent an active enzyme–substrate complex that could transfer hydrogen directly from substrate to coenzyme.

Recent studies indicate that hydrogen tunneling occurs during the oxidation of benzyl alcohol by horse liver and yeast alcohol dehydrogenases (Cha et al., 1989; Bahnson et al., 1993). For hydrogen tunneling to occur, the reactive carbons must be brought close together so that the classical energy barrier is penetrated (Klinman, 1991). Only dynamic fluctuations of the protein could bring the reactants closer than what is observed in the structure of the enzyme complexed with NAD^+ and pentafluorobenzyl alcohol.

The *p*-bromobenzyl alcohol binds in almost the same place as does pentafluorobenzyl alcohol, with its oxygen ligated to the catalytic zinc, but the different positions of the rings result in a different orientation of the *pro-R* hydrogen (Figure 8). For the bromo alcohol, a relatively small movement of the alcohol would place the *pro-R* hydrogen in proximity to the NAD^+. If the positions of the oxygen of the alcohol bound

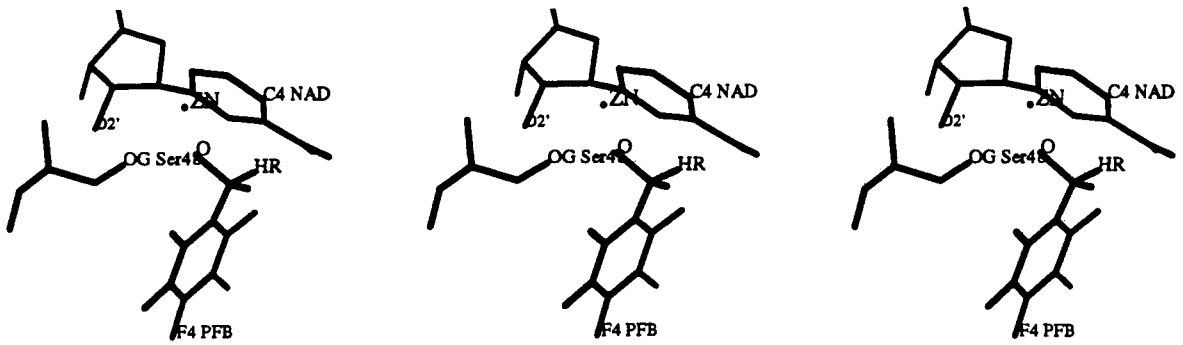

FIGURE 11: View of the active site of the monoclinic complex with pentafluorobenzyl alcohol. Hydrogens of the methylene carbon of the alcohol are indicated by lines, and the *pro-R* hydrogen is labeled.

to the catalytic zinc and the bromine in its pocket are maintained, rotation around the single bonds of the hydroxymethyl carbon (C7) produces a favorable orientation, with a C7–C4 distance of 3.4 Å. Thus, the results with the monoclinic enzyme confirm the previous conclusions with the triclinic form [Figure 6 in Eklund et al. (1982)].

The pentafluoro- and *p*-bromobenzyl alcohols bind in slightly different positions. However, it appears that the geometry of hydrogen transfer would be similar in both cases. Enzymes are dynamic molecules, and significant movements in the active site are energetically feasible. We suggest that the structures of these complexes approximate active complexes in the ground state.

REFERENCES

Anderson, D., & Dahlquist, F. W. (1980) *Biochemistry 19*, 5486–5493.

Bahnson, B., Park, D.-H., Kim, K., Plapp, B. V., & Klinman, J. P. (1993) *Biochemistry 32*, 5503–5507.

Baker, E. N., & Hubbard, R. E. (1984) *Prog. Biophys. Mol. Biol. 44*, 97–179.

Bignetti, E., Rossi, G. L., & Zeppezauer, E. (1979) *FEBS Lett. 100*, 17–22.

Birktoft, J. J., Fu, Z., Carnahan, G. E., Rhodes, G., Roderick, S. L., & Banaszak, L. J. (1989) *Biochem. Soc. Trans. 17*, 301–304.

Blum, M., Metcalf, P., Harrison, S. C., & Wiley, D. C. (1987) *J. Appl. Crystallogr. 20*, 235–242.

Bondi, A. (1964) *J. Phys. Chem. 68*, 441–451.

Brändén, C.-I., Jörnvall, H., Eklund, H., & Furugren, B. (1975) *The Enzymes (3rd ed.) 11*, 103–190.

Brünger, T. A., Kuriyan, J., & Karplus, M. (1987) *Science 235*, 458–460.

Cedergren-Zeppezauer, E., Samama, J.-P., & Eklund, H. (1982) *Biochemistry 21*, 4895–4908.

Cha, Y., Murray, C. J., & Klinman, J. P. (1989) *Science 243*, 1325–1330.

Cleland, W. W. (1992) *Biochemistry 31*, 317–319.

Colonna-Cesari, F., Perahia, D., Karplus, M., Eklund, H., Brändén, C.-I., & Tapia, O. (1986) *J. Biol. Chem. 261*, 15273–15280.

Creighton, D. J., Hajdu, J., & Sigman, D. S. (1976) *J. Am. Chem Soc. 98*, 4619–4625.

Dworschack, R. T., & Plapp, B. V. (1977) *Biochemistry 16*, 2716–2725.

Ehrig, T., Hurley, T. D., Edenberg, H. J., & Bosron, W. F. (1991) *Biochemistry 30*, 1062–1068.

Eklund, H., & Brändén, C.-I. (1987) in *Biological Macromolecules and Assemblies* (Jurnak, F. A., & McPherson, A., Eds.) Vol. 3, pp 74–142, John Wiley, New York.

Eklund, H., Nordström, Zeppezauer, E., Söderlund, G., Ohlsson, I., Boiwe, T., Söderberg, B.-O., Tapia, O., Brändén, C.-I., & Åkeson, Å. (1976) *J. Mol. Biol. 102*, 27–59.

Eklund, H., Samama, J.-P., Wallén, L., Brändén, C.-I., Åkeson, Å., & Jones, T. A. (1981) *J. Mol. Biol. 146*, 561–587.

Eklund, H., Plapp, B. V., Samama, J.-P., & Brändén, C.-I. (1982) *J. Biol. Chem. 257*, 14359–14358.

Eklund, H., Samama, J.-P., & Jones, T. A. (1984) *Biochemistry 23*, 5982–5996.

Engh, R. A., & Huber, R. (1991) *Acta Crystallogr. A47*, 392–400.

Filman, D. J., Bolin, J. T., Matthews, D. A., & Kraut, J. (1982) *J. Biol. Chem. 257*, 13663–13672.

Jones, T. A., Zou, J.-Y., Cowan, S. W., & Kjeldgaard, M. (1991) *Acta Crystallogr. A47*, 110–119.

Kvassman, J., & Pettersson, G. (1978) *Eur. J. Biochem. 87*, 417–427.

Klinman, J. P. (1991) in *Enzyme Mechanism from Isotope Effects* (Cook, P. F., Ed.) pp 127–148, CRC Press, Boca Raton, FL.

Laskowski, R. A., MacArthur, M. W., Moss, D. S., & Thornton, J. M. (1993) *J. Appl. Crystallogr. 26*, 283–290.

Lee, B. K., & Richards, F. M. (1971) *J. Mol. Biol. 55*, 379–400.

Matthews, B. W. (1993) *Annu. Rev. Biochem. 62*, 139–160.

Meyer, E. (1992) *Protein Sci. 1*, 1543–1562.

Nyburg, S. C., & Faerman, C. H. (1985) *Acta Crystallogr. B41*, 274–279.

Park, D.-H. (1991) Ph.D. Thesis, The University of Iowa, Iowa City, IA.

Pettersson, G. (1987) *CRC Crit. Rev. Biochem. 21*, 349–389.

Plapp, B. V., Eklund, H., & Brändén, C.-I. (1978) *J. Mol. Biol. 122*, 23–32.

Samama, J.-P. (1979) Ph.D. Thesis, Université Louis Pasteur de Strasbourg, Strasbourg.

Schneider, G., Cedergren-Zeppezauer, E., Knight, S., Eklund, H., & Zeppezauer, M. (1985) *Biochemistry 24*, 7503–7510.

Sekhar, V. C., & Plapp, B. V. (1990) *Biochemistry 29*, 4289–4295.

Shearer, G. L., Kim, K., Lee, K. M., Wang, C. K., & Plapp, B. V. (1993) *Biochemistry 32*, 11186–11194.

Skarżyński, T., Moody, P. C. E., & Wonacott, A. J. (1987) *J. Mol. Biol. 193*, 171–187.

Steitz, T. A. (1990) *Q. Rev. Biophys. 23*, 205–280.

Sund, H., & Theorell, H. (1963) *The Enzymes (2nd ed.) 7*, 25–83.

Teeter, M. M. (1991) *Annu. Rev. Biophys. Biophys. Chem. 20*, 577–600.

Theorell, H., & Yonetani, T. (1963) *Biochem. Z. 338*, 537–553.

Wratten, C. C., & Cleland, W. W. (1963) *Biochemistry 2*, 935–941.